Investigation of the Violation of the Lam-Tung Relation and the Difference in Angular Distribution in Quark-Antiquark and Quark-Gluon Production of Z Boson

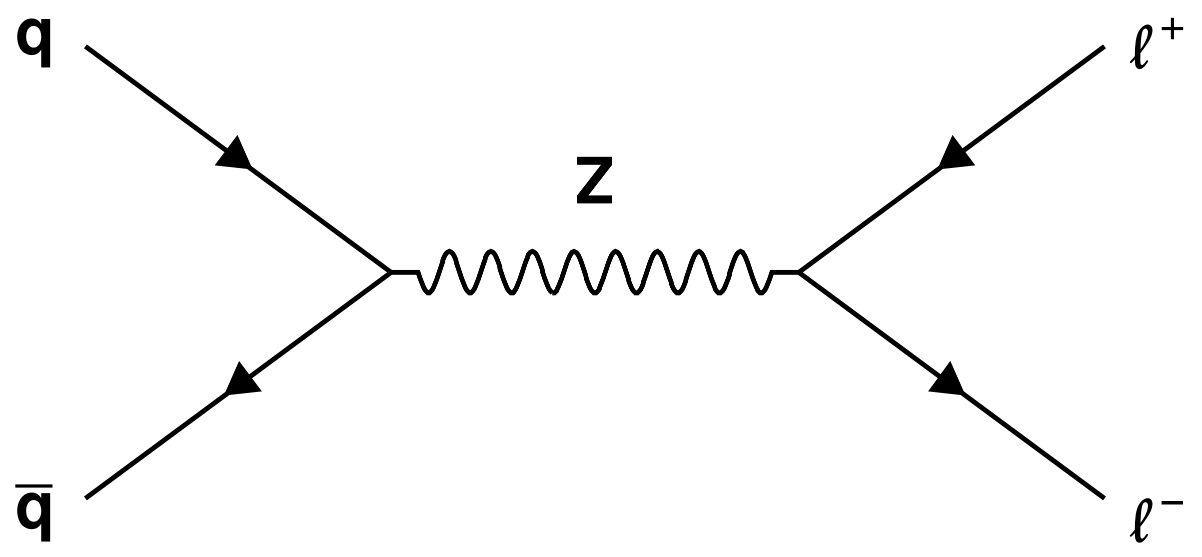

Giulia-Maria Bulugean

Prof. Arie Bodek, Prof. Aran Garcia-Bellido, Hyon San Seo, Rhys Taus

University of Rochester

PHENO 2026 - May 11th

Hard-scattering processes for Z → $\ell^+\ell^-$ at the LHC

Different initial states → different angular structures → test of the Lam–Tung relation.

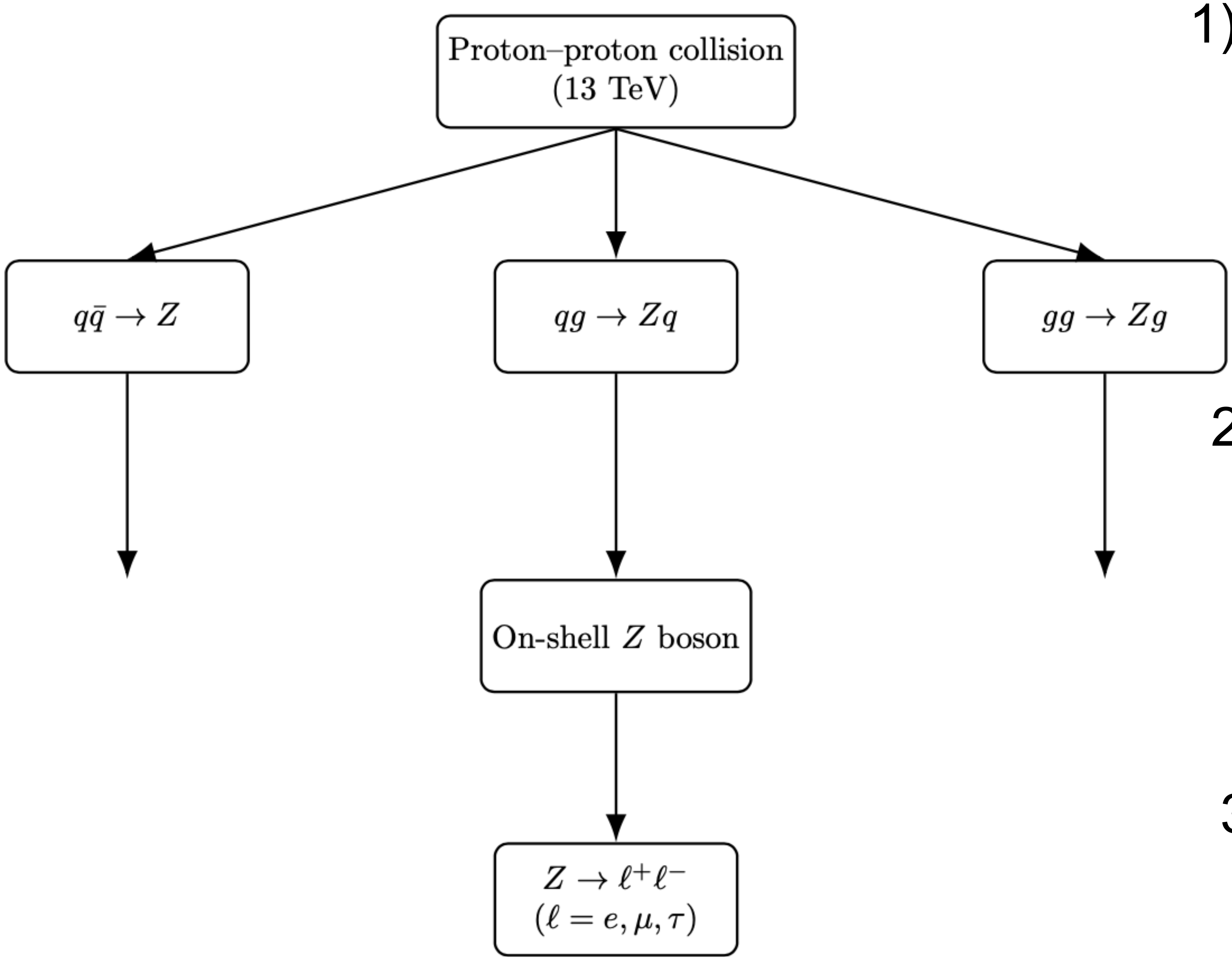

1) $q\bar{q} \to Z \to \ell^+\ell^-$

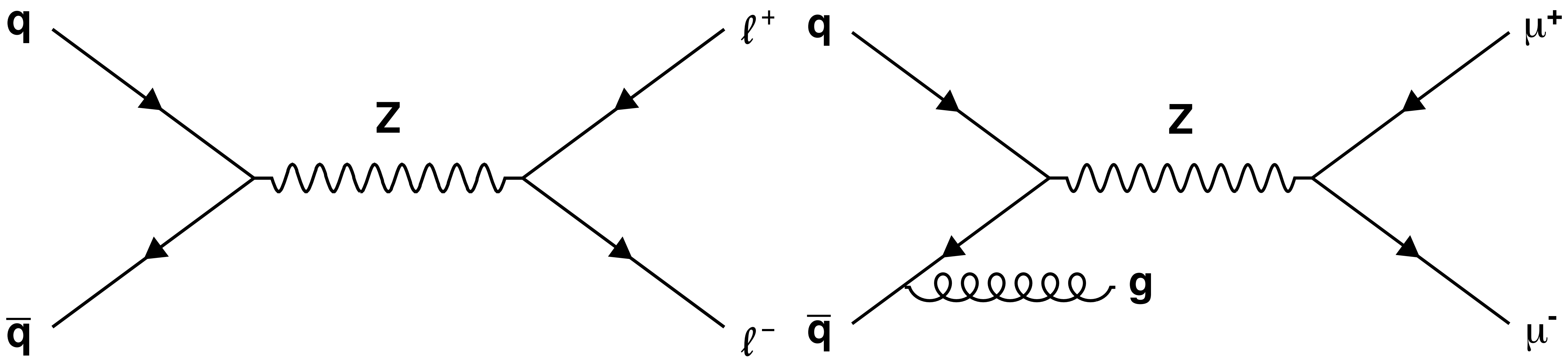

2) $qg \to Zq \to \ell^+\ell^- q$

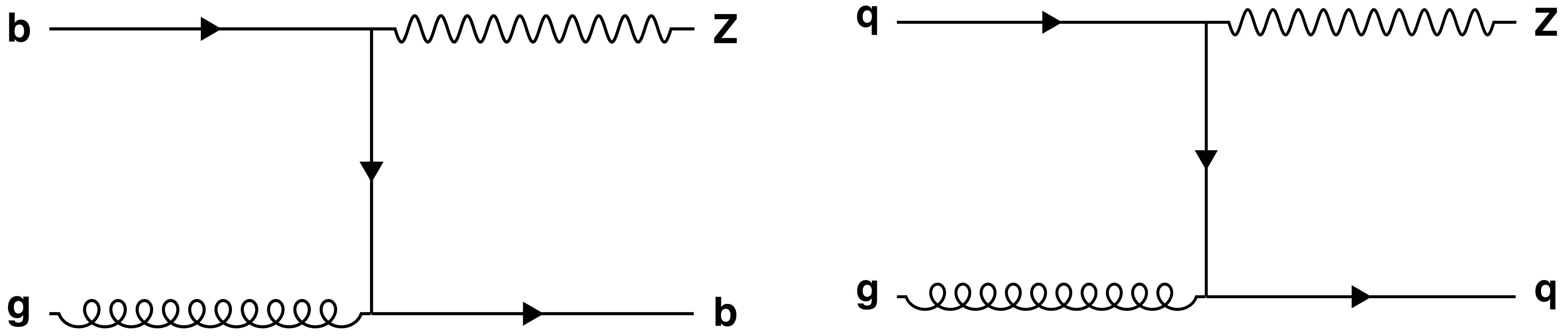

3) $gg \to Z q\bar{q}$

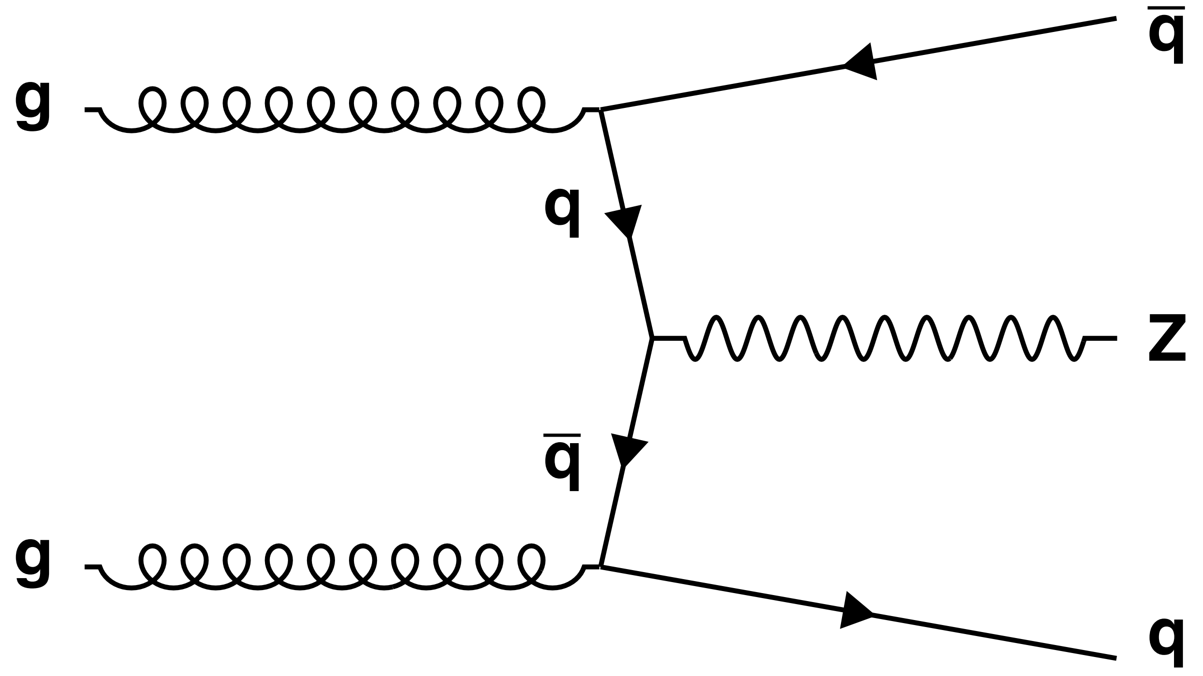

Lam-Tung relation

In Drell–Yan lepton pair production, the angular distribution of the leptons in the dilepton rest frame can be written as:

$$\frac{d\sigma}{d\Omega} \propto 1 + \cos^2\theta + \frac{1}{2}A_0(1 - 3\cos^2\theta) + \frac{1}{2}A_2 \sin^2\theta\cos 2\phi + \ldots$$

Where:

θ: polar angle of the lepton

ϕ: azimuthal angle

Integrating the distribution over φ and summing over ±cosθ leads to the 1D Collins–Soper polar distribution used to extract A_0.

The **Lam–Tung relation** is the theoretical prediction:

$$A_0 - A_2 = 0$$

C. S. Lam and W.-K. Tung, Phys. Rev. D 18, 2447 (1978).

at **leading order (LO)** in perturbative QCD for Drell–Yan production

Analysis Goals

- **Use Monte Carlo:** POWHEG-MiNNLO 2.0 for $pp \to Z \to \mu^+\mu^-$ interfaced to PYTHIA 8
- **Compare A_0 and A_2 between partonic initial states:** $q\bar{q},\ qg,\ gg$
- **Test the Lam-Tung relation $(A_0 - A_2 = 0)$ across different kinematic regions**
- **Event selection cuts:** $80 < M_Z < 100$ GeV, $p_T^{\text{jet}} > 20$ GeV, $|\eta_{\text{jet}}| < 2.4,\ \Delta R > 0.4$
- **Study dependence on jet multiplicity** (0-jet, 1-jet, 2-plus jets, inclusive)
- **Measure the angular coefficients A_0 and A_2 in Drell-Yan $Z \to \ell^+\ell^-$**
- **Validate results against theoretical predictions and PDF choices**
- **Use b-jets to select the QG process and study heavy-flavor contributions**

Lam-Tung relation

For $q\bar{q}$ process: $A_0^{q\bar{q}} = A_2^{q\bar{q}} = \dfrac{p_T^2}{M^2 + p_T^2}$ (valid for all orders)

For the Compton process: $gq \rightarrow Z/\gamma^*$,

A_0 and A_2 depend on the PDFs and rapidity y

At LO pQCD (after integrating over y): $A_0^{gq} = A_2^{gq} \approx \dfrac{5\, p_T^2}{M^2 + 5\, p_T^2}$

Since for the qg process the expression is only an approximation, we also developed an improved form and derived one for gg as well.

At higher orders, $A_2 < A_0$ because of multiple-jet emission (smearing in ϕ).

Experimentally for events with ≥ 2 jets, the Lam--Tung relation does not hold.

A0 and A2 at Gen Level

Angular distribution:

$$\frac{d\sigma}{d\Omega} \propto (1+\cos^2\theta)+\frac{1}{2}A_0(1-3\cos^2\theta)+\frac{1}{2}A_2 \sin^2\theta\cos 2\phi$$

- $\cos\theta$ distribution $\Rightarrow A_0$

Polar angular distribution $1D$ $(\cos\theta)$ *for* A_0:

$$\frac{d\sigma}{d\cos\theta} \propto (1+\cos^2\theta)+\frac{1}{2}A_0(1-3\cos^2\theta)$$

- $1D$ ϕ distribution $\Rightarrow A_2$

2D angular distribution $(\cos\theta, \phi)$ used for A_2:

$$\int d(\cos\theta)\frac{d^2\sigma}{d\cos\theta\, d\phi} \propto 1+\frac{A_2}{4}\cos 2\phi$$

$\min\chi^2$

$$\chi^2(N, A_0) = \sum_i \frac{\left[n_i^{(\theta)} - N\left((1+x_i^2)+\frac{1}{2}A_0(1-3x_i^2)\right)\right]^2}{\sigma_i^2}$$

$$x_i \equiv \cos\theta_i$$

$n_i^{(\theta)}$ =content of bin i in the $|\cos\theta|$ histogram.

$$\chi^2(N, A_2) = \sum_i \frac{\left[n_i^{(\phi)} - N\left(1+\frac{1}{4}A_2\cos 2y_i\right)\right]^2}{\sigma_i^2}$$

$$y_i \equiv \phi_i$$

$n_i^{(\phi)}$ = bin i in the ϕ distribution

Fraction of events across QQbar, QG and GG processes

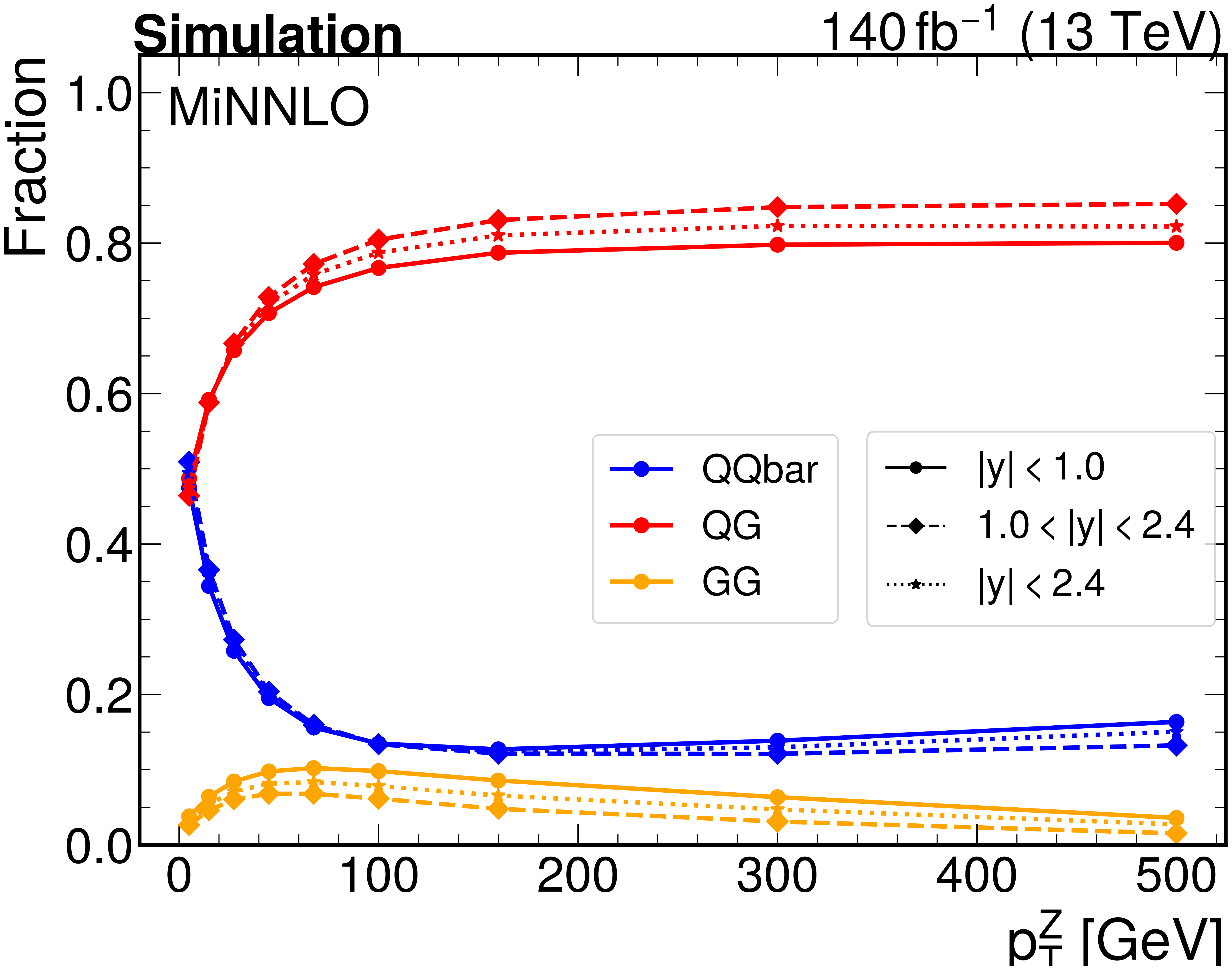

- qG dominates the sample, rising from ~50% at low p_T^Z to ~80% at high p_T^Z; q$\bar{q}$ decreases and GG stays small
- The q$\bar{q}$, qG, and GG fractions are very similar in all three rapidity regions.
- We therefore focus on |Y| < 2.4, which gives the widest rapidity coverage and largest event sample.

Moments Method

- We use 3 2D histograms (absY x p_T):

  $w(|y|, p_T)$ -> total event weight

  $a_0(|y|, p_T)$ -> sum of w_i f_0 (θ_i, ϕ_i)

  $a_2(|y|, p_T)$ -> sum of w_i f_2 (θ_i, ϕ_i)

- Integrate over the 2D maps (absY x pT) over the chosen rapidity range (|y|<1.0 or 1.0<|y|<2.4)

$$\text{moment} = \frac{\sum_i w_i f_i}{\sum_i w_i} \qquad r_0(p_T) = \frac{\sum_i w_i\, f_0(\theta_i, \phi_i)}{\sum_i w_i} \qquad r_2(p_T) = \frac{\sum_i w_i\, f_2(\theta_i, \phi_i)}{\sum_i w_i}$$

- Compute normalized moments

$$r_0(p_T) = \frac{a_0(p_T)}{w(p_T)}, \qquad r_2(p_T) = \frac{a_2(p_T)}{w(p_T)}$$

- Convert moments to angular coefficients

$$A_0(p_T) = \frac{2}{3} + \frac{20}{3}\, r_0(p_T) \qquad A_2(p_T) = 20\, r_2(p_T)$$

Moments vs Fitting Method & Rapidity

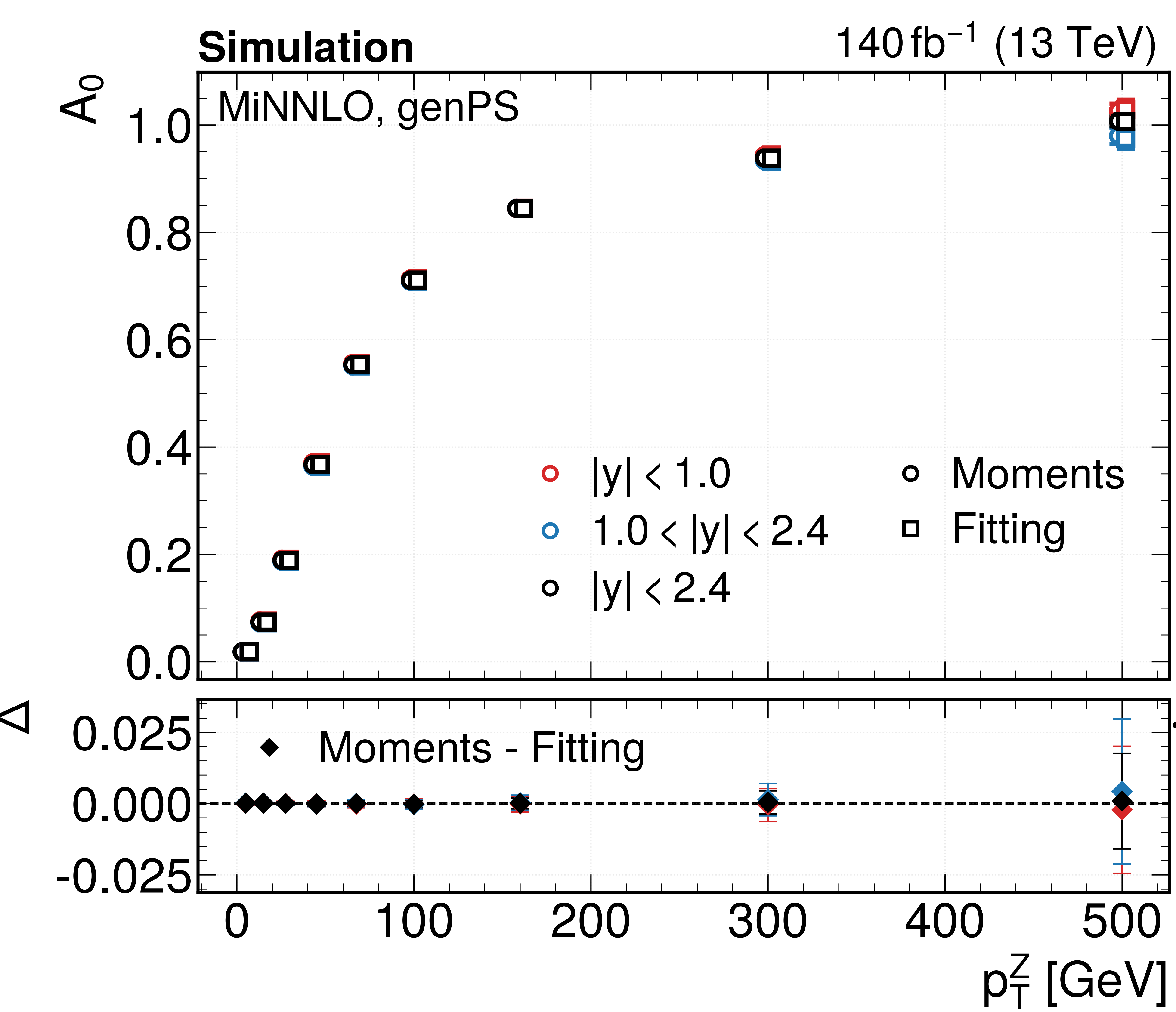

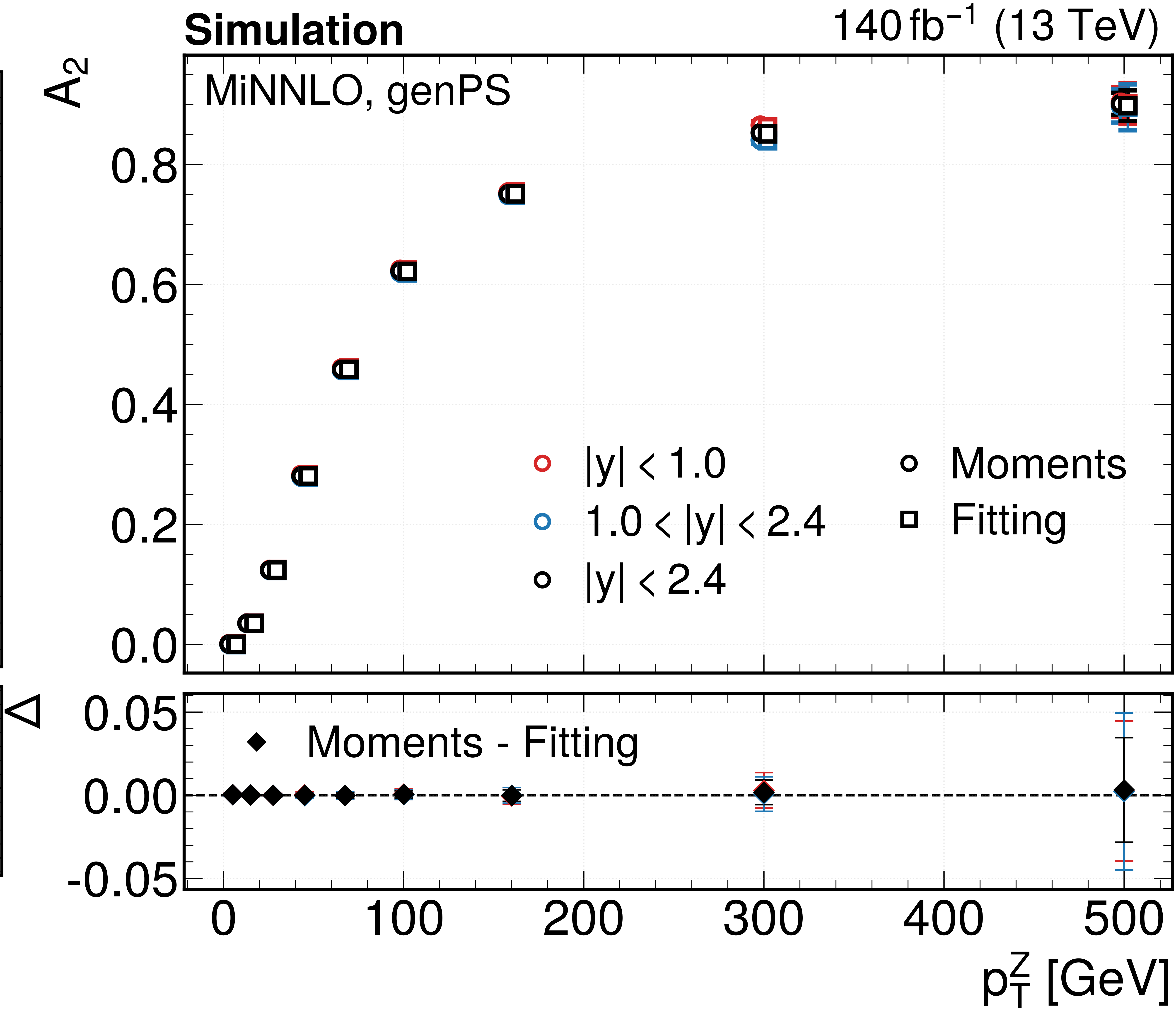

Moments vs Fitting Method & Rapidity

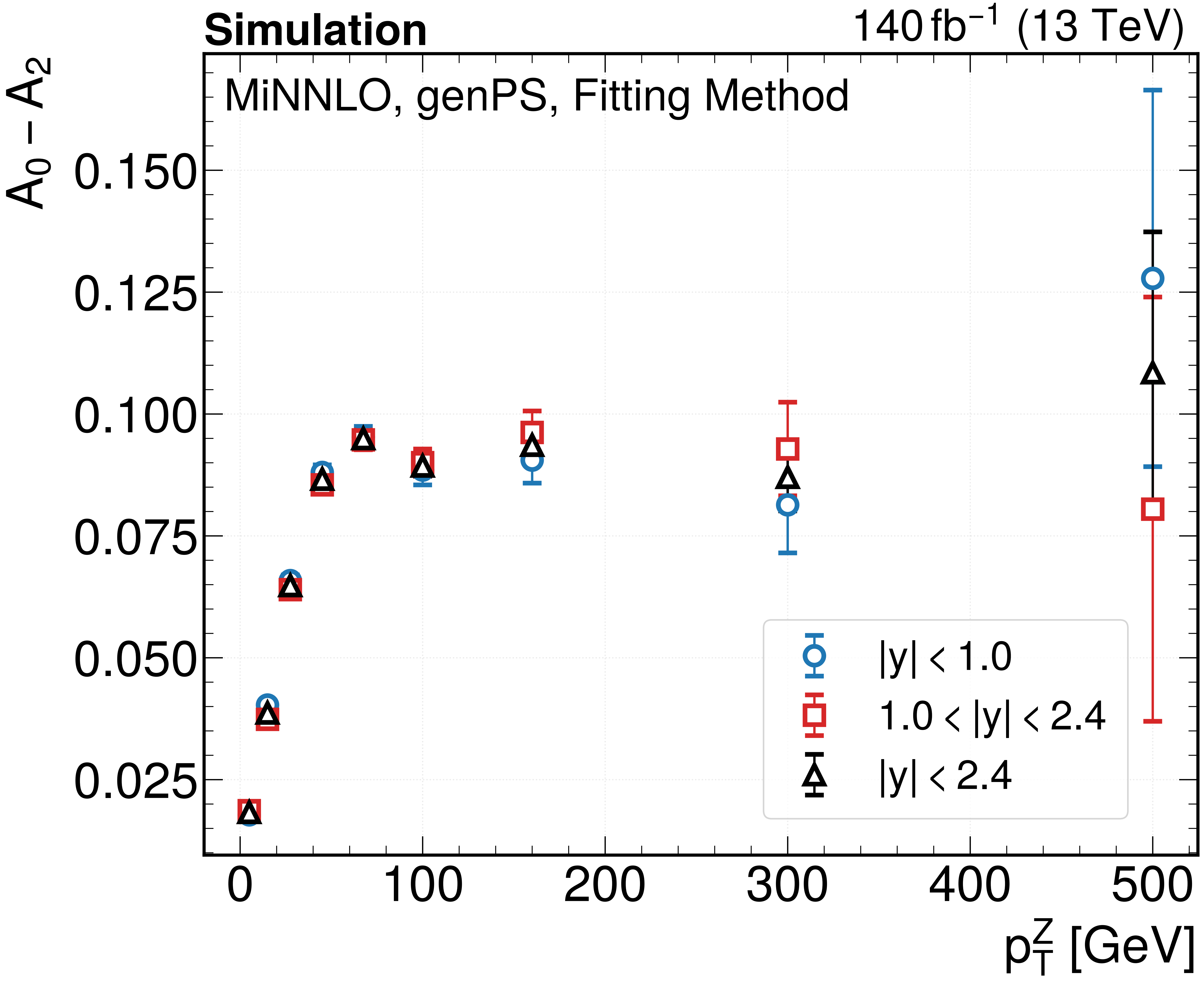

- In each (p_T^Z, |Y|) bin, the moments method extracts A0 and A2 from event-by-event angular weights.
- The fit method extracts bin-integrated A0 and A2 from the 1D |cosθ| and 2D ($\cos^2\theta$, $\sin^2\phi$) distributions.
- The two methods agree within uncertainties, validating the fit method for the rest of the analysis.
- A0, A2, and A0−A2 are consistent across all three rapidity regions, motivating the focus on |Y|<2.4 in the rest of the study

Extraction of A0 and A2 at Generator Level
all jets included vs events with LE 1 jet, all processes ($q\bar{q}$, qG, GG)

A0-A2 at Generator Level

all jets included vs events with LE 1 jet, all processes (qq̄, qG, GG)

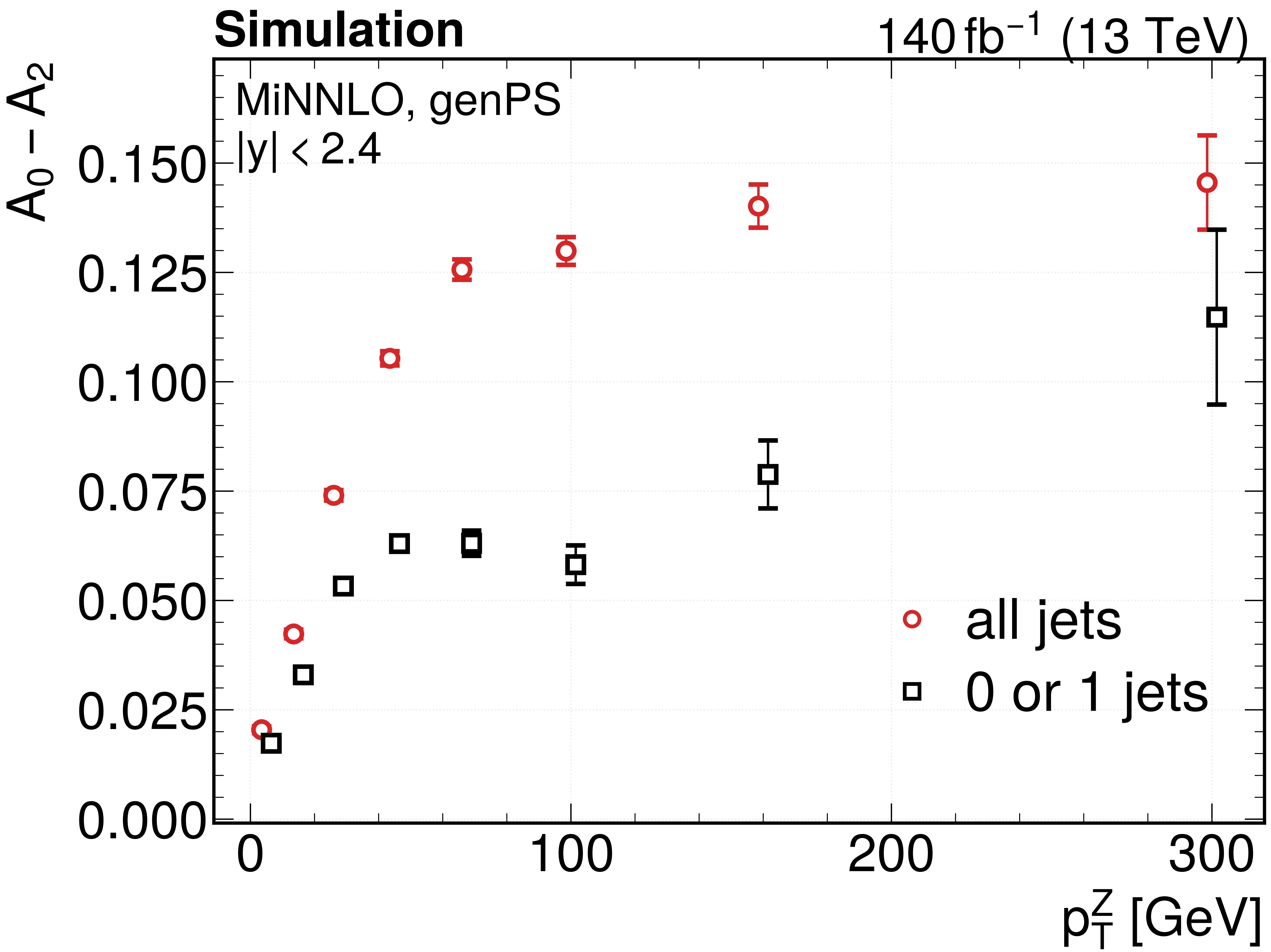

- In the inclusive sample, A_2 is below A_0 at moderate and high $p_T{}^Z$, showing clear Lam–Tung violation.
- For 0 or 1 jet events ($p_T{}^{jet}$ > 20 GeV, |η^{jet}| < 2.4), A_0 and A_2 become much closer and $A_0 - A_2$ is reduced close to 0.
- This indicates that the violation is driven mainly by multijet events.
- The likely origin is extra hard radiation, which smears the ϕ distribution and lowers A_2 relative to A_0.

Extraction of A0 at Generator Level
QQbar only

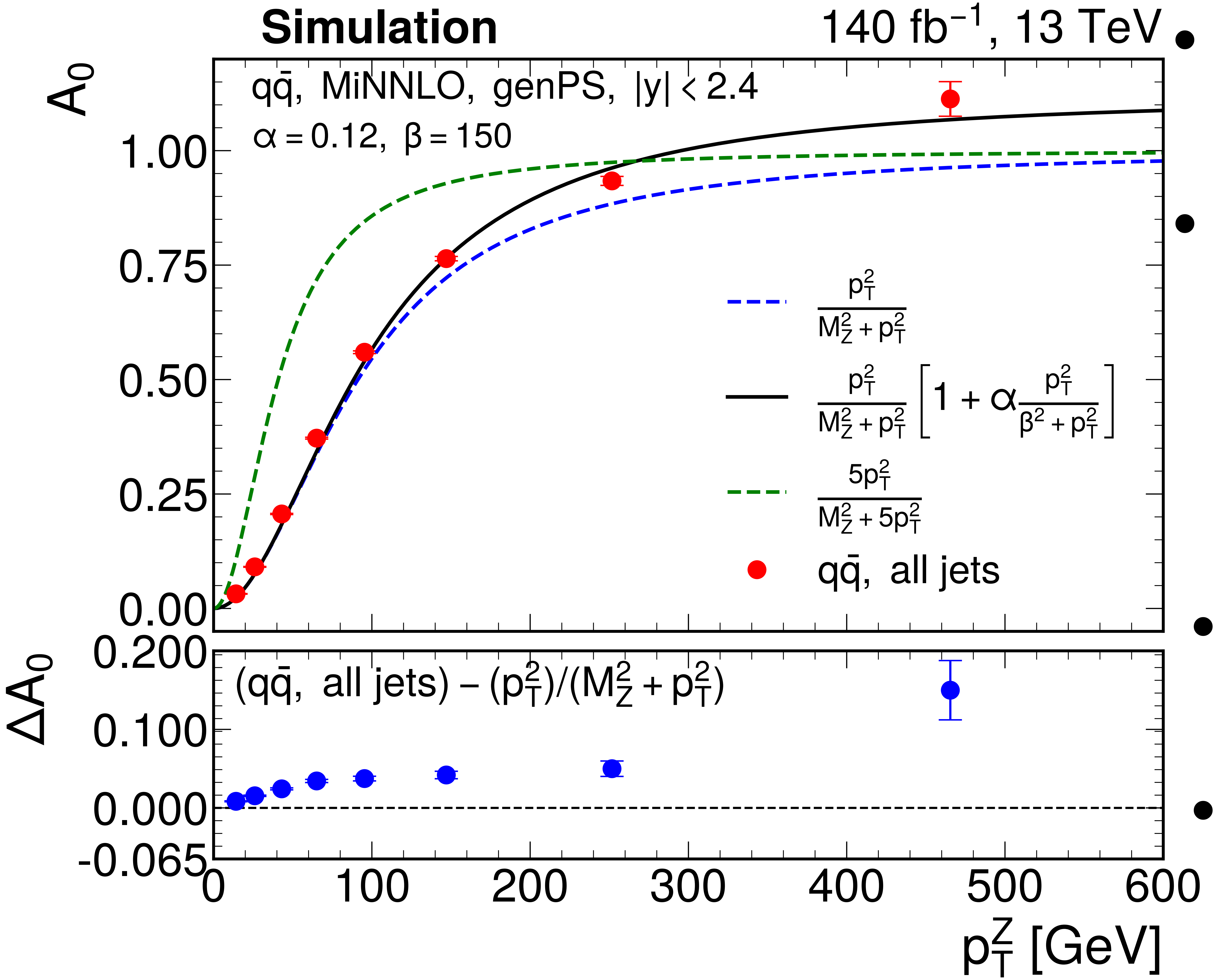

- For $q\bar{q}$, the standard prediction $p_T^2/(M_Z^2 + p_T^2)$ already describes A0 well at low and moderate p_T^Z.
- At high p_T^Z, the MC predicts a slightly larger A0 than this simple form.

$$A_0^{q\bar{q}}(p_T) = \frac{p_T^2}{M_Z^2 + p_T^2}\left(1 + \alpha\,\frac{p_T^2}{\beta^2 + p_T^2}\right)$$

$$\alpha \approx 0.12,\ \beta \approx 150\ \text{GeV}$$

- This excess comes from multiple gluon emissions by both the quark and antiquark in the same event.
- The improved form works better because it preserves the low-p_T behavior and adds a smooth high-p_T enhancement.

Improved Prediction for A_{qg}

- Small-p_T limit: $A_0 \to 0$ as $p_T^Z \to 0$
- Large-p_T limit: $A_0 \to 1$ (dominantly transverse polarization at high recoil)

Classical Approximation for QG processes:

$$A_{0,qg}^{\text{old}}(p_T) \approx \frac{5\,p_T^2}{M_Z^2 + 5\,p_T^2}$$

Improved prediction : keeps $A_0(0) \approx 0$ and $A_0(\infty) \approx 1$, but allows shape flexibility .

$$A_0^{\text{improved}}(p_T; \alpha, C) = \alpha\,\frac{5\,p_T^2}{M_Z^2 + 5\,p_T^2} + (1-\alpha)\,\frac{C\,p_T^2}{M_Z^2 + C\,p_T^2}, \qquad 0 \le \alpha \le 1,\; C > 0$$

- α : mixing between the classic QG curve ($\kappa = 5$) and an adjustable shape .
- C : controls how fast A_0 rises with p_T .

Same strategy is applied for deriving a prediction for GG processes

Extraction of A0 at Generator Level
QG only

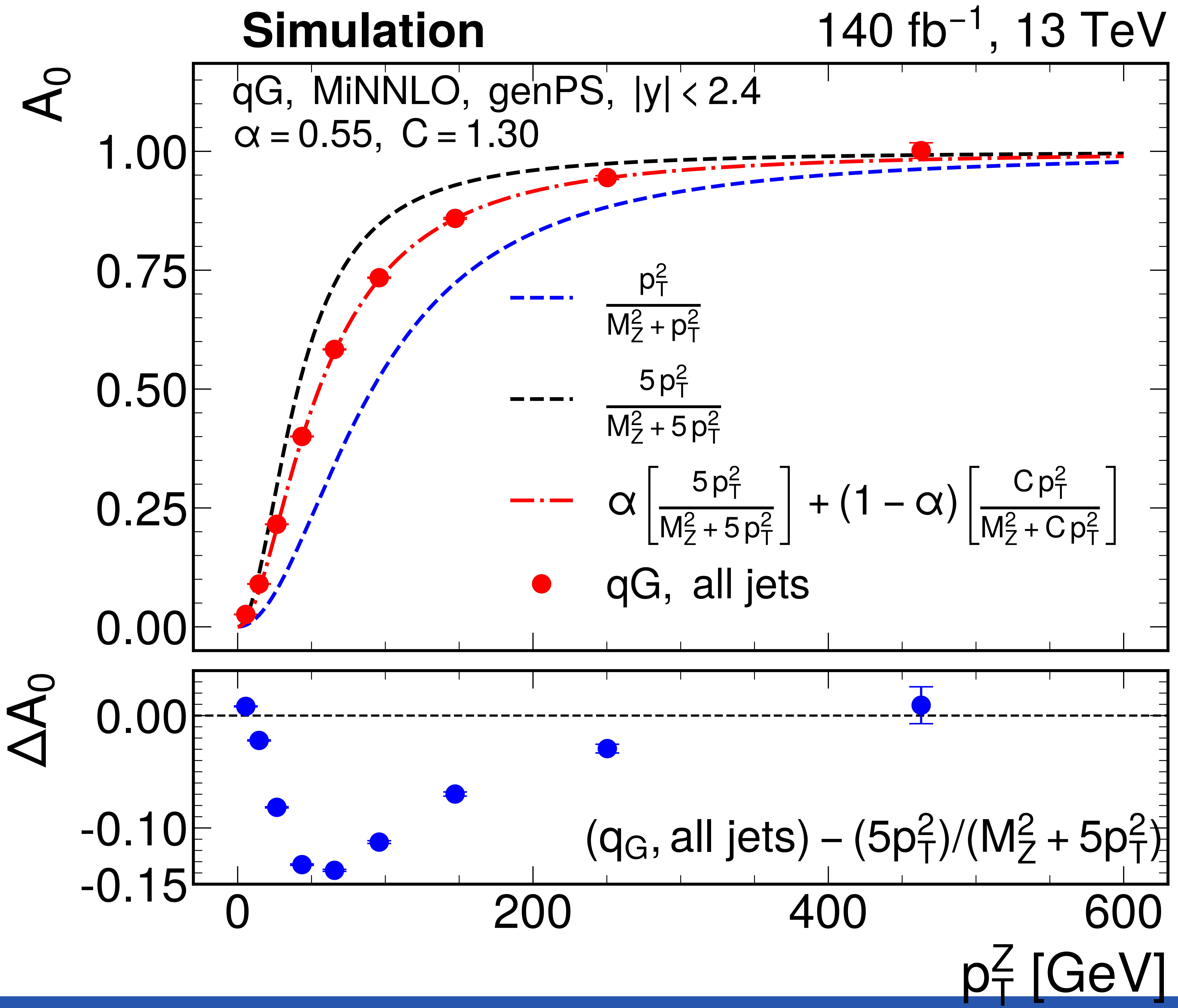

- For qG - approximation $5p_T^2/(M_Z^2 + 5p_T^2)$ overestimates A0, especially at intermediate and high p_T^Z.
- This form is derived at leading order, with one hard parton recoiling against the Z; in that limit the Z is nearly transversely polarized, so A0 rises too quickly toward 1

$$A_0^{qG}(p_T) = \alpha \frac{5p_T^2}{M_Z^2 + 5p_T^2} + (1-\alpha)\frac{Cp_T^2}{M_Z^2 + Cp_T^2}$$

$$\alpha \approx 0.55, \qquad C \approx 1.30$$

- The improved form mixes the qG - approximation curve with a second, more flexible term.
- It keeps the correct limits, A0 → 0 at low p_T and A0 → 1 at high p_T

Extraction of A0 at Generator Level
GG only

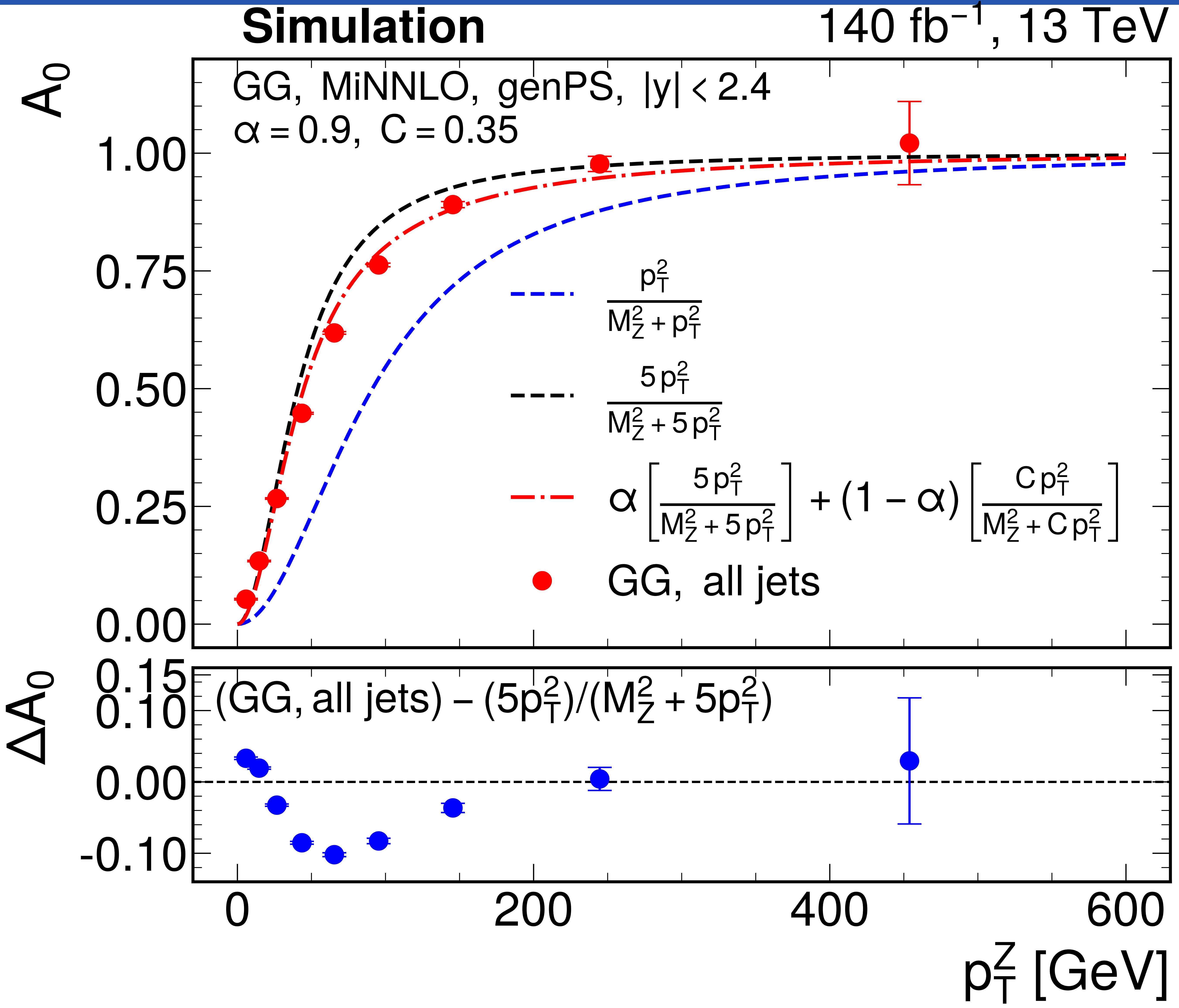

- For GG -approximation $5p_T^2/(M_Z^2 + 5p_T^2)$ also overestimates A0, most clearly at intermediate p_T^Z.
- As for qG, this form comes from a simple LO picture and rises too quickly toward A0 = 1 compared with the full GG simulation.
- The improved form mixes the standard curve with a second term that allows a slower rise.

$$A_0^{GG}(p_T) = \alpha \frac{5p_T^2}{M_Z^2 + 5p_T^2} + (1-\alpha)\frac{Cp_T^2}{M_Z^2 + Cp_T^2}$$

$$\alpha \approx 0.9, \qquad C \approx 0.35$$

Using events with a single B-tagged jet to measure A_0^{qG}

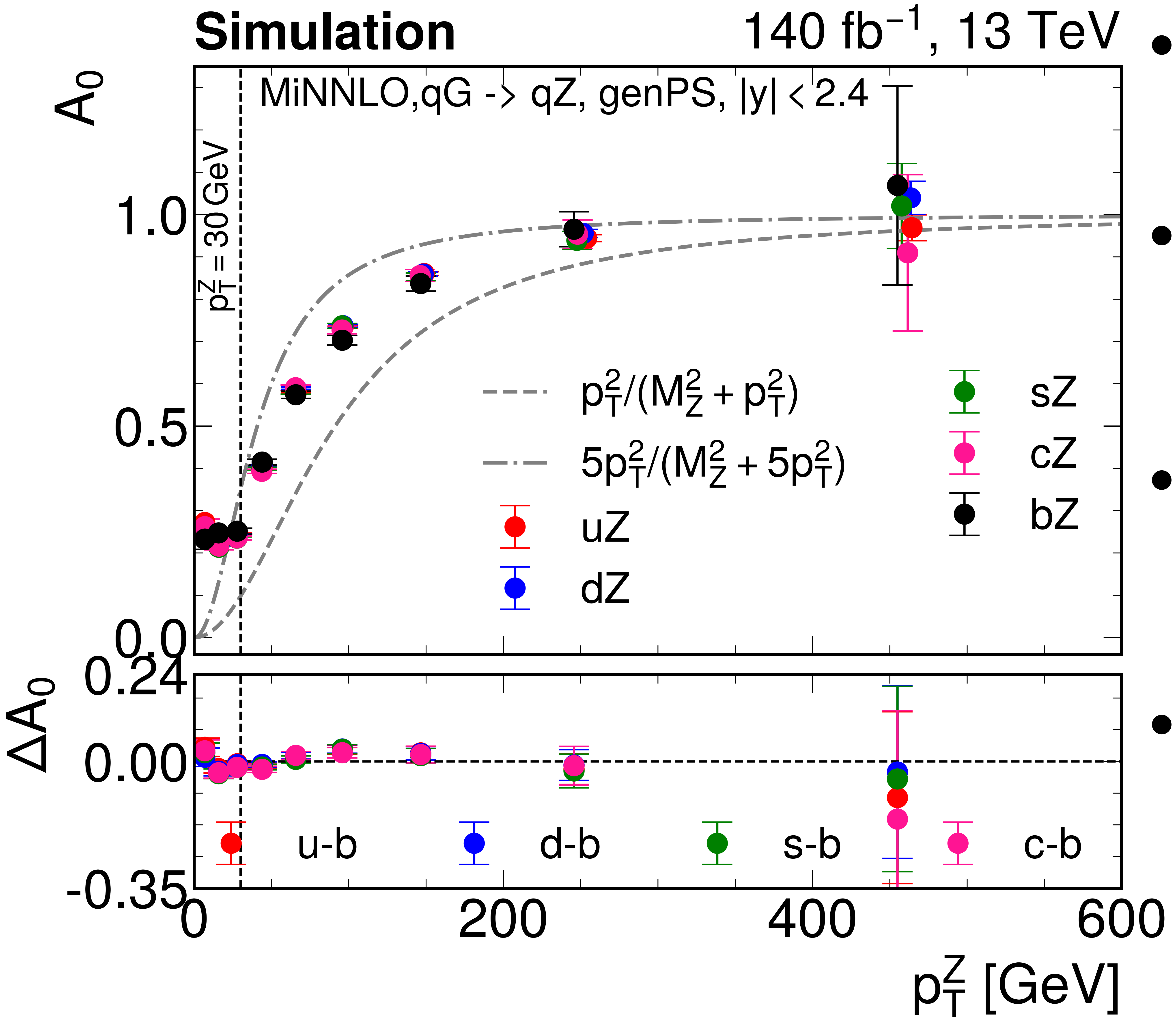

- All five quark flavors give almost identical A0(p_T^Z) curves, so the qG + b-jet handle has very small flavor/PDF dependence.
- It's expected that heavier c and b quarks to change A0, but their mass and PDF differences only weakly affect the distributions compared to the overall qG kinematics.
- As a result, the A0 shape is effectively universal across flavors, which lets us use a single b-tagged jet to select a clean qG sample with little flavor bias.
- We apply a b-jet p_T >20 GeV cut so focus on p_T^Z > 30 GeV, where the dynamics are more perturbative and jets are well reconstructed, avoiding the collinear region that complicates A0 at very low p_T^Z.

Using events with a single B-tagged jet to measure A_0^{qG}

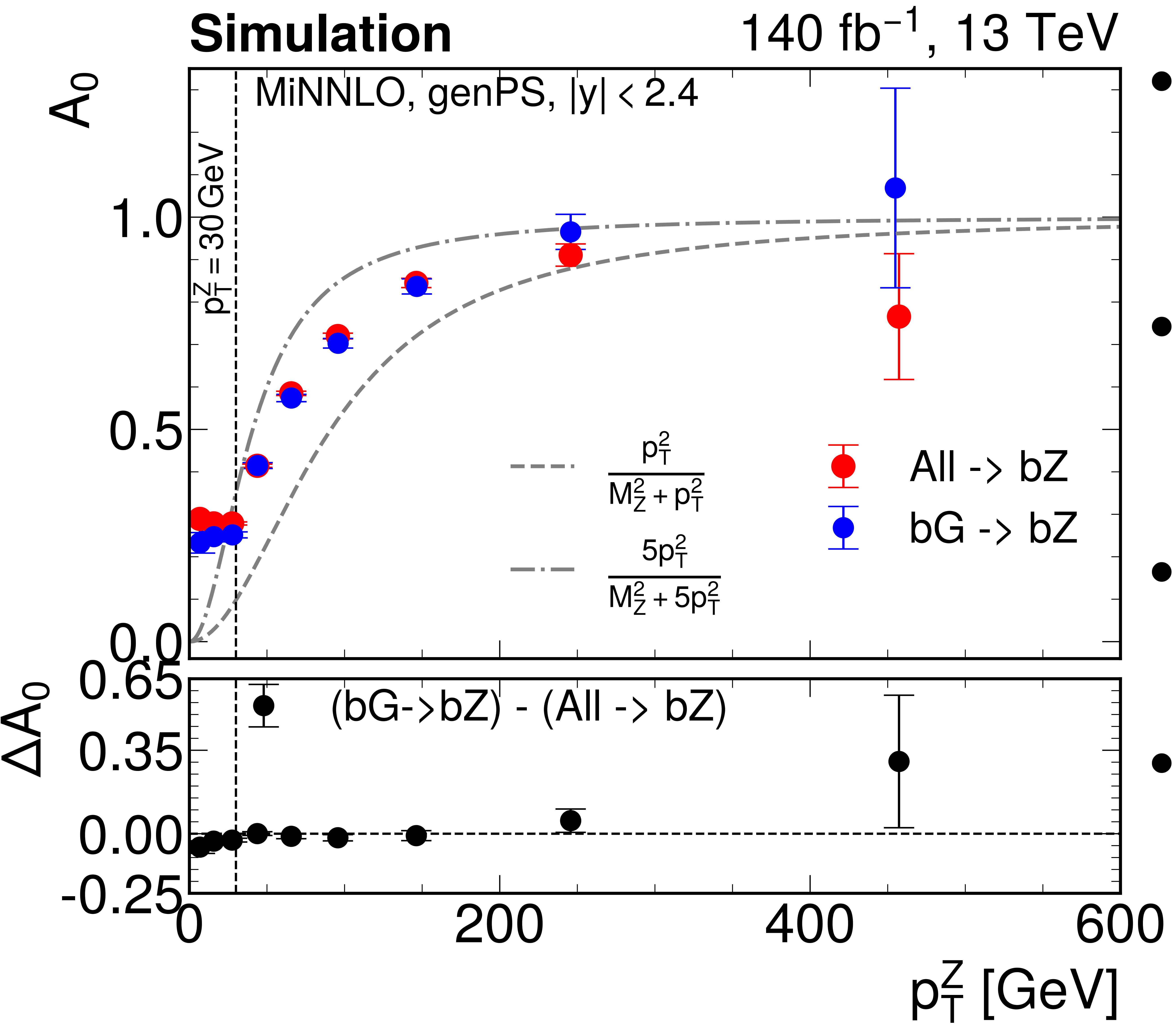

- This plot compares A0 for all → bZ events and for the true bG → bZ subset; above $p_T^Z \approx 30$ GeV the two are consistent within uncertainties.
- The small ΔA0 between these samples shows that a single b-tagged jet already selects a sample that is highly enriched in qG → bZ events.
- Experimentally: we cannot isolate the qG process directly, but using b-jets gives us an indirect way to measure A0 for qG.
- Therefore, measuring A0 in events with exactly one b-tagged jet provides a practical handle to study A_0^{qG} over most of the accessible p_T^Z range.

Conclusions

- At 13 TeV, Z production is dominated by gluon-initiated processes; the $q\bar{q}$ channel contributes only about 40% of the cross section in the Z-mass window.

- Using MiNNLO, we show that the Lam–Tung violation A0 − A2 mainly arises from events with more than one jet, while samples with at most one jet remain close to A0 = A2.

- We provide empirical parametrizations that accurately describe A0 for $q\bar{q}$, qG, and GG over the full pTZ range, improving over the classic geometric and $5p_T^2/(M^2+5p_T^2)$ forms.

$$A_0^{q\bar{q}}(p_T^Z) = \frac{(p_T^Z)^2}{M_{\mu\mu}^2 + (p_T^Z)^2}\left[1 + \alpha\,\frac{(p_T^Z)^2}{\beta^2 + (p_T^Z)^2}\right]$$

$$\alpha \approx 0.30, \qquad \beta \approx 150\ \text{GeV}$$

$$A_0^{X}(p_T^Z) = \alpha\,\frac{5\,(p_T^Z)^2}{M_{\mu\mu}^2 + 5\,(p_T^Z)^2} + (1-\alpha)\,\frac{C\,(p_T^Z)^2}{M_{\mu\mu}^2 + C\,(p_T^Z)^2}$$

$$\alpha_{qG} \approx 0.55, \qquad C_{qG} \approx 1.30$$

$$\alpha_{GG} \approx 0.90, \qquad C_{GG} \approx 0.35$$

- Finally, we demonstrate that events with a single b-tagged jet offer an experimentally feasible way to isolate the qG contribution and test these predictions for $A0^{qG}$ at the LHC.

Thank you!

Back-up slides

Particle ID(s) and Notation

gg: $\text{gen\_id}_1 = 21 \;\wedge\; \text{gen\_id}_2 = 21$

qg: $\left(|\text{gen\_id}_1| \in \{1,\ldots,6\} \;\wedge\; \text{gen\_id}_2 = 21\right) \;\vee\; \left(|\text{gen\_id}_2| \in \{1,\ldots,6\} \;\wedge\; \text{gen\_id}_1 = 21\right)$

Notation:

- nJets0or1: events with 1 or less jets
- nJets_inclusive: all events regardless of their jet multiplicity
- QQbar/ QG/ GG: events obtained only through QQbar/ QG/ GG processes

LHE information: the parton-level event record from the hard matrix-element calculation before any parton showering or hadronization is applied

PS information: the event after QCD parton showering (and typically hadronization), where additional soft/collinear radiation is generated, giving a more realistic final-state structure.

Analysis Binning

- Z-boson p_T bins (GeV): (0,10), (10,20), (20,35), (35,55), (55,80), (80,120), (120,200), (200,400)
- Rapidity bins : $|y| \in [(0.0,1.0), (0.0,2.4)]$

  Today's talk is mostly focused on the rapidity bin corresponding to abs(y)<1
- Angular variables (Collins--Soper):

  $|\cos\theta_{CS}| \in [0,1]$, $|\phi_{CS}| \in [0,\pi]$,
- 2D angular maps: 48×48 bins for $|\cos\theta|$ and $|\phi|$
- Response matrices (per p_T bin): 10×10 bins in $|\cos\theta|$ and $|\phi|$

Acceptance Cuts

We're using MINNLO sample with NNPDF31_nnlo_hessian_pdfas

All the following cuts are specifically for the dimuon channel

- $80 < m_{\ell\ell} < 100\,\text{GeV}$ (Z-peak mass window)
- Jets: $p_T^{\text{jet}} > 20\,\text{GeV},\ |\eta^{\text{jet}}| < 2.4$
- $\Delta R(\ell, \text{jet}) > 0.4$ (lepton--jet overlap removal)
- b-tagging: accounting for incoming and outgoing b-quarks

Re-weighting Procedure for A0 and A2

- **Forward folding:**

  Apply the normalized response matrix $\widehat{R}$ to the reweighted gen-level templates.

  Predict the Reco-level distributions: $\mathbf{m}(A) = \widehat{R}\,\mathbf{g}(A)$

- **Projection to 1D:**

  Sum over ϕ $\rightarrow$ Reco $\cos\theta$ spectrum for A_0

  Sum over $\cos\theta$ $\rightarrow$ Reco ϕ spectrum for A_2

- **Comparison with data:**

  Compare predictions with Reco data.

$$\chi^2(A) = \sum_i \frac{(D_i - s\,m_i(A))^2}{D_i}$$

- **Fit procedure:**

  Coarse scan of trial values.

  Refined minimization near best value.

$i \in \{1,\ldots,10\}$ (reco bin index in ϕ or $\cos\theta$)

D_i = observed reco bin content (data or MC)

$$s(A) = \frac{\sum_i D_i}{\sum_i m_i(A)} \quad (\textit{normalization factor})$$

$m_i(A)$ = model prediction in bin i for trial parameter A

Re-weighting Procedure for A0 and A2 Templates Method

Inputs:

- Truth-level angular templates $(\cos\theta,\ \phi)$ from simulation
- Measured angular distributions from data (Reco level)
- Response matrix describing how detector effects smear truth into measured quantities

- **Angular dependence:**

$$\frac{d\sigma}{d\cos\theta} \propto 1 + \cos^2\theta + \frac{A_0}{2}(1 - 3\cos^2\theta)$$

- **Template reweighting:**

$$w(\cos\theta) = \frac{1 + \cos^2\theta + \frac{A_0^{\text{new}}}{2}(1 - 3\cos^2\theta)}{1 + \cos^2\theta + \frac{A_0^{\text{nom}}}{2}(1 - 3\cos^2\theta)}$$

- **Angular dependence:**

$$\frac{d\sigma}{d\phi} \propto 1 + \frac{A_2}{4}(1 - 2\sin^2\phi)$$

- **Template reweighting:**

$$w(\phi) = \frac{1 + \frac{A_2^{\text{new}}}{4}(1 - 2\sin^2\phi)}{1 + \frac{A_2^{\text{nom}}}{4}(1 - 2\sin^2\phi)}$$